JACS
JOURNAL OF THE AMERICAN CHEMICAL SOCIETY
Communication
pubs.acs.org/JACS

A Catalyst Selection Protocol That Identifies Biomimetic Motifs from β-Hairpin Libraries

Masaomi Matsumoto,[†] Stephen J. Lee,[‡] Marcey L. Waters,*[,†] and Michel R. Gagné*[,†]

[†]Department of Chemistry, University of North Carolina at Chapel Hill, Chapel Hill, North Carolina 27599-3290, United States
[‡]U.S. Army Research Office, P.O. Box 12211, Research Triangle Park, North Carolina 27709, United States

Supporting Information

ABSTRACT: Assaying a solid-phase library of histidine-containing β-hairpin peptides by a reactive tagging scheme in organic solvents selects for catalysts that reproduce the strategies used by His-based enzyme active sites to accelerate acyl- and phosphonyl-transfer reactions. Rate accelerations (k_{rel}) in organic solvents of up to 2.4×10^8 are observed.

Enzymes have evolved a number of related strategies to accelerate the numerous acylation/deacylation and phosphorylation/dephosphorylation reactions on which life depends. Conserved in the active site of these enzymes is a nucleophilic or basic histidine that acts in concert with other residues to activate acyl/phosphoryl reactants (amides, esters, ATP, etc.). For example, the His/Ser combination is ubiquitous in the serine proteases,[1] His/Asp in ribonuclease, malate dehydrogenase, and phospholipase A,[2] and His/His in paraoxonase.[3] Mechanistically, histidine may play the role of the nucleophile or the base that activates a key nucleophile (e.g., serine, water), with both approaches achieving potent enzyme rate accelerations (up to 10^{10}).[1,4] We aim to use any combination of these generic strategies, and either nucleophilic or basic mechanisms to achieve high rates of acyl-transfer catalysis (e.g., Scheme 1).

Scheme 1

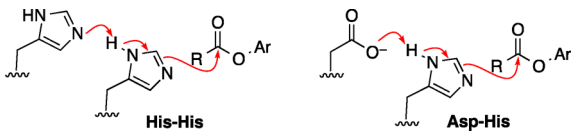

The incorporation of both β and non-natural peptide turn elements can be effective for structuring peptides to achieve high (enantio)*selectivities* in peptide-catalyzed reactions, acyl-transfer reactions by *N*-alkyl histidines in organic solvents and as ligands in palladium-catalyzed allylation being noteworthy examples.[5,6] The challenge of achieving high *reactivities* with synthetic enzyme mimics, however, has been met comparatively rarely.[7] Part of the reason may be that synthetic enzyme mimics lack much of the complexity of enzymes. Approaches to solving this dilemma include rigid scaffolds with defined structures[8] as well as solid-phase libraries of structurally diverse peptides.[9] On the other hand, random screening of large peptide libraries does not necessarily provide potential catalysts with functionality that is organized in an active-site-like arrangement. With the explicit goal of high rates, we have sought to bridge this gap through libraries of structured peptides capable of nucleating active-site-like structures.

We have previously developed a reactive tagging scheme to screen helical peptides and, in so doing, discovered catalysts capable of large rate accelerations for acyl-transfer reactions ($V_{rel} = V_{cat}/V_{uncat}$ up to 2800).[10] As we report herein, extending these studies to the β-hairpin scaffold has provided catalysts with V_{rels} up to 44 000 (2.5 mM catalyst) and $k_{rel} = k_{cat}/k_{uncat}$ up to 2.4×10^8, and, most importantly, provided insights into the role of functional group cooperativity in catalysis. The β-hairpin scaffold displays ordered side chains with multiple close contacts, both with a residue's ±2 neighbors in the linear sequence and those laterally and diagonally across the strand (Figure 1).[11]

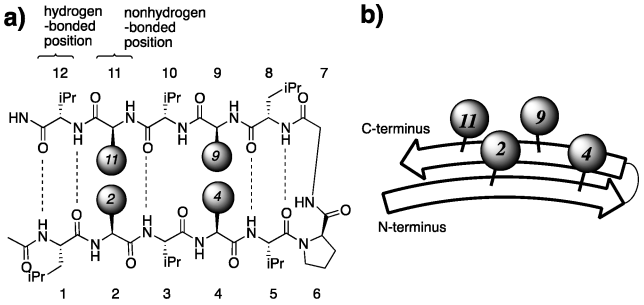

Figure 1. (a) β-Hairpin structure showing H-bonded (HB) and non-H-bonded (NHB) faces of a 12-mer β-hairpin. (b) Schematic showing interdigitation of residues on the NHB face.

As previously described, the reactive tagging assay identifies peptides that rapidly generate the *N*-acyl His intermediate. Under nucleophile-free conditions, this intermediate is stable and thereby enables a colored acylating agent[12] to visually tag hyperactive components in a one-bead, one-compound format (Scheme 2).

The peptide scaffold was designed to display His and multiple variable units on the non-H-bonded face of the β-hairpin while keeping the H-bonded face residues constant to help fold into the desired structure (Figure 1).[13] The side chains on the non-H-bonded face pack closely and interdigitate with the cross-strand residues,[13,14] a situation we considered

Received: March 27, 2014
Published: October 27, 2014

dx.doi.org/10.1021/ja503012g | J. Am. Chem. Soc. 2014, 136, 15817−15820

Scheme 2. Deprotonation of the *N*-Acylimidazolium Intermediate Tags the Hit as a Neutral *N*-Acylimidazole

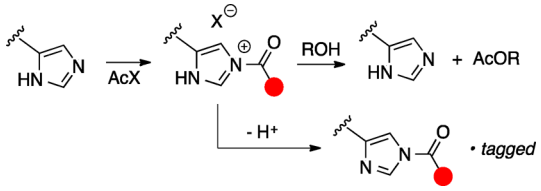

especially conducive to facilitating cooperative side-chain interactions.

The libraries consisted of 8- or 12-residue peptides that numbered in the hundreds or low thousands, with variable residues (both natural and unnatural) at the non-H-bonded positions of the β-hairpin. Aromatic, hydrogen-bond-donating, hydrogen-bond-accepting, and hydrophobic residues were included. Residues known to stabilize the β-hairpin structure were incorporated in the H-bonded positions,[13] and a dPro-Gly turn sequence was included to template folding into a β-hairpin.[15] The reactive tagging was performed in CH_2Cl_2 under conditions that were adjusted to achieve <5% of visibly colored beads at the end of the assay (see Supporting Information (SI) for details). Physical separation of the dye-tagged beads and photocleavage for MALDI-MS analysis provided hit candidates that were resynthesized by standard solid-phase peptide synthesis (SPPS) methods for subsequent kinetic analysis. Sequence ambiguities were resolved by parallel SPPS of all possible isomers and side-by-side dye-tagged testing (see SI). Once the optimal sequence isomer was identified in this manner, it was synthesized by SPPS, isolated, and purified for kinetic testing.

The reaction in eq 1 proved useful for kinetic analysis, as its background rate is slow and it can be monitored by both ^{1}H

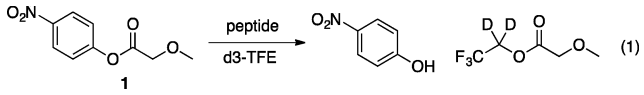

NMR and UV–vis spectroscopy. Across the spectrum of libraries that were screened, selected, and tested for catalytic competence, those achieving a V_{rel} > 10 000 at 2.5 mM catalyst are collected in Scheme 3a.[16] Expressed as a concentration-independent ratio of second-order rate constants,[17] $k_{rel} = k_{cat}/k_{uncat}$, the rate accelerations reach as high as 2.4×10^8 (Scheme 3, see SI for details).[18]

For eq 1, this hit set provides a suggestive view of the features that contribute to high activity, as each His can partner to create a non-covalent dyad, triad, or tetrad that structurally resembles histidine-activating arrangements in a variety of enzymes. The bis-His and tris-His hits, **HWWH** and **HWHH**[19] (where the hit name corresponds to the residues on the non-H-bonding face making up the catalytic site from the N- to C-terminus), resemble the reactive His-His dyad in the active site of paraoxonase, where one histidine increases the basicity of the second (Scheme 1). Such a mechanism has been proposed for the imidazole-catalyzed hydrolysis of esters, which displays second-order kinetic behavior in catalyst.[20] The emergence of multi-His hits implies that this mode of action may be providing a kinetic benefit to β-hairpin structures, which through side-chain interdigitation can accommodate closely interacting His residues.

Scheme 3. (a) Hit Peptides Identified by Reactive Tagging, with V_{rel} >10 000, and (b) Control Peptides

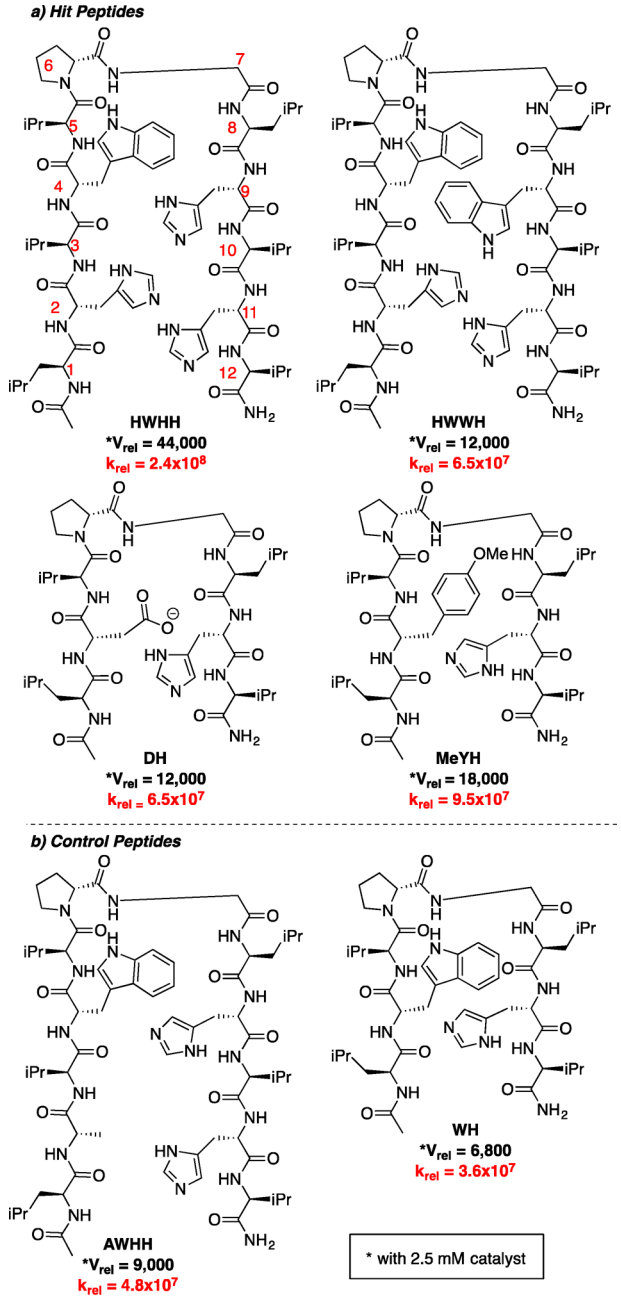

Two additional hits emerged from the competitive screening protocol: the **DH** catalyst, which displays a cross-strand Asp-His arrangement and parallels the His-activation mode displayed by enzymes like ribonuclease, and the **MeYH** hit, which displays an aromatic residue cross strand to the His. Interestingly, three of the top four catalysts have an aromatic residue terminating the chain of His residues. Since cross-strand aromatic pairs interact edge to face,[13,14] it may be that the aromatic residue helps orient the catalytic functional groups.[21] Additionally, cation–π interactions between a putative imidazolium ion and the aromatic residue may help stabilize positive charge buildup along the reaction coordinate.[21] Although the precise role of the Asp-His dyad in active sites is debated,[22] it is conceivable that, in the present case, it may be acting to bias His into a reactive tautomer, to stabilize a

dx.doi.org/10.1021/ja503012g | J. Am. Chem. Soc. 2014, 136, 15817–15820

developing imidazolium ion, or both.[23] Regardless of the mode of action, the results of our screening exercise demonstrate that His-His, His-π, and His-Asp dyads, and by extension their non-covalent interactions, are privileged for accelerating acyl-transfer catalysis.

Although the parallels to established motifs for active-site His activation suggest biomimetic mechanisms, we sought supporting evidence for the role of non-covalent interactions in catalyst structure and activity. The top catalyst in the collection, **HWHH**, was selected for additional study, particularly focusing on the chain of His residues and the potential for cooperative interactions on His activation. Consistent with the structure in Figure 1, circular dichroism (CD) spectroscopy, along with α and amide proton chemical shifts, supported a β-hairpin structure (Figures 10−13-SI), while 2D NMR revealed extensive NOE crosspeaks between tryptophan and histidine side chains in support of an interdigitated network (Figures 16−21-SI). Alternative arrangements of three His residues and one Trp on the face of the β-hairpin (**WHHH**, **HHWH**, and **HHHW**) were less active, indicating that a sequence-specific arrangement of side chains is optimal for catalysis. The protonation state of the active catalyst was determined to be neutral, as **HWHH·H**$^+$ was inactive for catalysis.[24] Monitoring the deprotonation of **HWHH·H**$^+_3$ with Et_3N revealed a positionally selective deprotonation (Figure 2), indicative of

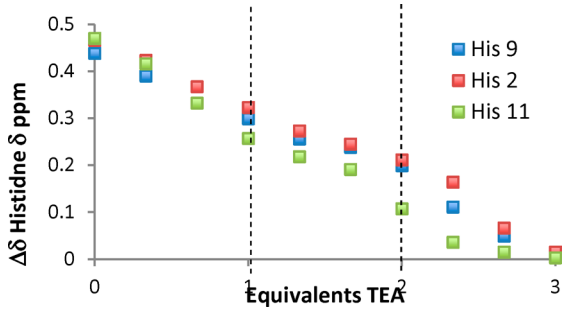

Figure 2. His 2, 9, and 11 δ proton chemical shifts during titration of **HWHH·H**$^+_3$ with Et_3N in TFE-d_3.

colocalization of the His residues and the potential for cooperativity. The role of the tris-His array in the kinetics of acyl transfer was additionally probed with control peptide **AWHH**, which replaces His-2 with alanine and disrupts the interdigitated network (Scheme 3b). **AWHH** displayed folding behavior by CD and NMR virtually identical to that of **HWHH** (Figures 10, 14, and 15-SI). The ∼5-fold drop in catalytic activity coupled with the even greater loss when two His units are removed (**WH**) suggests that the network of non-covalent interactions in peptides like **HWHH** is required for high activity.

In contrast to the behavior of **HWHH**, the deprotonation of **AWHH·H**$^+_2$ reveals no positional selectivity; i.e., each histidine behaves independently (Figure 7-SI). This suggests disruption of the H-bond network, which is also consistent with the lack of NOEs between side chains on the NHB face in **AWHH**.

A similar titration of **DH·H**$^+$ with Et_3N confirms that the aspartic acid deprotonates first (Figure 3), but its β-CH continues to shift upfield during the phase of the titration when His becomes deprotonated. This sensitivity suggests that, at neutral pH, a significant interaction occurs between aspartate and *imidazolium*, consistent with the scenario in Scheme 1.

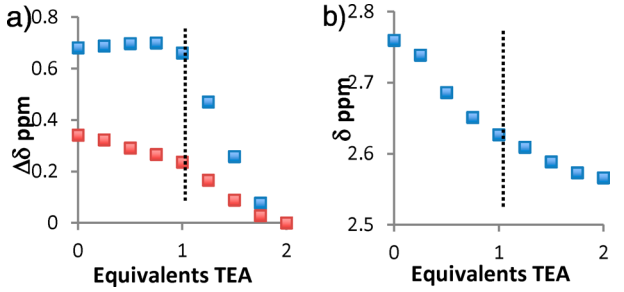

Figure 3. (a) Imidazole ε (blue) and δ (red) chemical shifts during titration of **DH·H**$^+$ with Et_3N. (b) Aspartic acid β chemical shift during Et_3N titration of **DH·H**$^+$.

This collection of hit and control peptide catalysts provides unique insights into the structural features that create high activity on the β-hairpin scaffold. Under competitive selection conditions, features that code for cooperative behavior with an active-site His emerge from the library. Although our mechanistic data are circumstantial, the structural parallels to active-site mechanisms in acyl- and phosphoryl-transfer enzymes coupled with high hit activities are striking and speak to the ability of the β-hairpin scaffold to support and display active-site-like structures. Several models of the Asp-His couple have been reported in aqueous media;[25] however, the kinetic advantages observed in those systems were surprisingly small. This work is the first example described in an organic solvent, which is relevant to the dielectric environment of enzyme active sites.[26] The absolute rate accelerations of these minimalist peptide catalysts are among the highest that have been observed.

■ ASSOCIATED CONTENT

Supporting Information

Experimental and characterization details and spectral data, including Figures 1−30-SI and Tables 1−3-SI. This material is available free of charge via the Internet at http://pubs.acs.org.

■ AUTHOR INFORMATION

Corresponding Authors

mlwaters@unc.edu
mgagne@unc.edu

Notes

The authors declare no competing financial interest.

■ ACKNOWLEDGMENTS

For financial support, M.R.G. and M.L.W. acknowledge the Defense Threat Reduction Agency (HDTRA1-10-1-0030), S.J.L. acknowledges the Army Research Office, and M.M. acknowledges a postdoctoral fellowship from the NRC.

■ REFERENCES

(1) (a) Hedstrom, L. *Chem. Rev.* **2002**, *102*, 4501−4523. (b) Ekici, O. D.; Paetzel, M.; Dalbey, R. E. *Protein Sci.* **2008**, *17*, 2023−2037.
(2) (a) Quirk, D. J.; Raines, R. T. *Biophys. J.* **1999**, *76*, 1571−1579. (b) Birktoft, J. J.; Banaszak, L. J. *J. Biol. Chem.* **1982**, *258*, 472−482. (c) van den Bergh, C. J.; Slotboom, A. J.; Verheji, H. M.; de Haas, G. H. *J. Cell. Biochem.* **1989**, *39*, 379−390.
(3) Khersonsky, O.; Tawfik, D. S. *J. Biol. Chem.* **2006**, *281*, 7649−7656.
(4) (a) Gutteridge, A.; Thornton, J. M. *Trends Biochem. Sci.* **2005**, *30*, 622−629. (b) Bartlett, G. J.; Porter, C. T.; Borkakoti, N.; Thornton, J. M. *J. Mol. Biol.* **2002**, *324*, 105−121. (c) Quezada, C. M.; Hamel, D. J.;

Gradinaru, C.; Bilwes, A. M.; Dahlquist, F. W.; Crane, B. R.; Simon, M. I. *J. Biol. Chem.* **2005**, *280*, 30581−30585.
(5) (a) Miller, S. J.; Copeland, G. T.; Papaioannou, N.; Horstmann, T. E.; Ruel, E. M. *J. Am. Chem. Soc.* **1998**, *120*, 1629−1630. (b) Miller, S. J. *Acc. Chem. Res.* **2004**, *37*, 601−610. (c) Davie, E. A. C.; Mennen, S. M.; Xu, Y.; Miller, S. *Chem. Rev.* **2007**, *107*, 5759−5812. (d) Gilberton, S. R.; Collibee, S. E.; Agarkov, A. *J. Am. Chem. Soc.* **2000**, *122*, 6522−6523.
(6) Muller, C. E.; Zell, D.; Hrdina, R.; Wende, R. C.; Wanka, L.; Schuler, S. M. M.; Schreiner, P. R. *J. Org. Chem.* **2013**, *78*, 8465−8484.
(7) (a) Copland, G. T.; Miller, S. J. *J. Am. Chem. Soc.* **2001**, *123*, 6496−6502. (b) Fierman, M. B.; O'Leary, D. J.; Steinmetz, W. E.; Miller, S. J. *J. Am. Chem. Soc.* **2004**, *126*, 6967−6971. (c) Evans, J. W.; Fierman, M. B.; Miller, S. J.; Ellman, J. A. *J. Am. Chem. Soc.* **2004**, *126*, 8134−8135.
(8) Kheirabadi, M.; Celebi Oelcuem, N.; Parker, M. F. L.; Zhao, Q. Q.; Kiss, G.; Houk, K. M.; Schafmeister, C. E. *J. Am. Chem. Soc.* **2012**, *134*, 18345−18353.
(9) (a) De Muynck, H.; Madder, A.; Farcy, N.; De Clercq, P. J.; Perez-Payan, M. N.; Ohberg, L. M.; Davis, A. P. *Angew. Chem.* **2000**, *39*, 145−148. (b) Krattinger, P.; McCarthy, C.; Pfaltz, A.; Wennemers, A. *Angew. Chem., Int. Ed.* **2003**, *42*, 1722−1724. (c) Schmuck, C.; Michels, U.; Dudaczek. *J. Org. Biomol. Chem.* **2009**, *7*, 4362−4368. (d) Clouet, A.; Darbre, T.; Reymond, J.-L. *Angew. Chem., Int. Ed.* **2004**, *43*, 4612−4615. (e) Albada, H. B.; Liskamp, R. M. J. *J. Comb. Chem.* **2008**, *10*, 814−824. (f) Revell, J. D.; Wennemers, H. *Curr. Opin. Chem. Biol.* **2007**, *11*, 269−278.
(10) Bezer, S.; Matsumoto, M.; Lee, S. J.; Gagné, M. R.; Waters, M. L. *Org. Biomol. Chem.* **2014**, *12*, 1488−1494.
(11) Syud, F. A.; Stanger, H. E.; Gellman, S. H. *J. Am. Chem. Soc.* **2001**, *123*, 8667−8677.
(12) A *p*-Nitrophenyl ester derivative of disperse red, 4-nitrophenyl-5-{*N*-ethyl-*N*-[4-(4-nitrophenyl)azo]phenyl}amino-3-oxapentanoate was used: Madder, A.; Farcy, N.; Hosten, N. G. C.; De Muynck, H.; De Clercq, P. J.; Barry, J.; Davis, A. P. *Eur. J. Org. Chem.* **1999**, 2787−2791.
(13) (a) Mahalakshmi, R.; Raghothama, S.; Balaram, P. *J. Am. Chem. Soc.* **2006**, *128*, 1125−1138. (b) Mahalakshmi, R.; Shanmugam, G.; Polavarapu, P. L.; Balaram, P. *ChemBioChem* **2005**, *6*, 2152−2158.
(14) (a) Tatko, C. D.; Waters, M. L. *J. Am. Chem. Soc.* **2002**, *124*, 9372−9373. (b) Tatko, C. D.; Waters, M. L. *J. Am. Chem. Soc.* **2004**, *126*, 2028−2034.
(15) (a) Haque, T. S.; Gellman, S. H. *J. Am. Chem. Soc.* **1997**, *119* (9), 2303−2304. (b) Stanger, H. E.; Gellman, S. H. *J. Am. Chem. Soc.* **1998**, *120* (17), 4236−4237.
(16) This concentration (2.5 mM) enabled kinetic and NMR data to be obtained under the same conditions.
(17) Ema, T.; Tanida, D.; Matsukawa, T.; Sakai, T. *Chem. Commun.* **2008**, 957−959.
(18) By comparison, *N*-boc-histidine methyl ester has a V_{rel} of 400.
(19) **HWHH** and **HWWH** peptides were selected from a 1296-member library; **MeYH** was selected from a 100-member library.
(20) Neuvonen, H. *J. Chem. Soc., Perkin Trans. 2* **1990**, 669−673.
(21) Matsumoto, M.; Lee, S. J.; Gagné, M. R.; Waters, M. L. *Org. Biomol. Chem.* **2014**, *12*, 8711−8718.
(22) (a) Blow, D. M. *Acc. Chem. Res.* **1976**, *9*, 145−152. (b) Cleland, W. W.; Frey, P. A.; Gerlt, J. A. *J. Biol. Chem.* **1998**, *273*, 25529−25532. (c) Schutz, C. N.; Warshel, A. *Proteins: Struct., Funct., Bioinf.* **2004**, *55*, 711−723. (d) Schafer, S. L.; Barrett, W. C.; Kallarakal, A. T.; Mitra, B.; Kozarich, J. W.; Gerlt, J. A.; Clifton, J. G.; Petskop, G. A.; Kenyon, G. L. *Biochemistry* **1996**, *35*, 5662−5669. (e) Schultz, L. W.; Quirk, D. J.; Raines, R. T. *Biochemistry* **1998**, *37*, 8886−8898. (f) Sprang, S.; Standing, S.; Fletterick, R. J.; Stroud, R. M.; Finer-Moore, J.; Xuong, N. H.; Hamlin, R.; Rutter, W. J.; Craik, C. S. *Science* **1987**, *237*, 905−909. (g) Craik, C. S.; Roczniak, S.; Largman, C.; Rutter, W. J. *Science* **1987**, *237*, 909−913. (h) Cosgrove, M. S.; Gover, S.; Naylor, C. E.; Vandeputte-Rutten, L.; Adams, M. J.; Levy, H. R. *Biochemistry* **2000**, *39*, 15002−15011.
(23) A reviewer suggested that catalysis by **DH** might proceed via an aspartate mixed anhydride, whose subsequent acyl transfer was catalyzed by histidine general base catalysis. Preliminary data are best rectified by a nucleophilic mechanism: (1) An *N*-acylimidazole intermediate forms from **DH** and **1** in the absence of nucleophile. (2) This intermediate reacts with trifluoroethanol. (3) A solvent kinetic isotope effect of 1.5 is inconsistent with a general base mechanism. See: Bender, M. L.; Bergeron, R. J.; Komiyama, M. *The Bioorganic Chemistry of Enzymatic Catalysis*; Wiley-interscience: New York, 1984; pp 45, 130.
(24) In contrast, previously reported His-His catalysis shows bell-shaped pH dependence, indicative of general acid catalysis. (a) Broo, K. S.; Nilsson, H.; Nilsson, J.; Flodberg, A.; Baltzer, L. *J. Am. Chem. Soc.* **1998**, *120*, 4063−4068. (b) Nicoll, A. J.; Allemann, R. K. *Org. Biomol. Chem.* **2004**, *2*, 2175−2180.
(25) (a) Komiyama, M.; Bender, M. L.; Utaka, M.; Takeda, A. *Proc. Natl. Acad. Sci. U.S.A.* **1977**, *74*, 2634−2638. (b) Zimmerman, S. C.; Cramer, K. D. *J. Am. Chem. Soc.* **1988**, *110*, 5906−5908. (c) Cramer, K. D.; Zimmerman, S. C. *J. Am. Chem. Soc.* **1990**, *112*, 3680−3682. (d) Zimmerman, S. C.; Korthals, J. C.; Cramer, K. D. *Tetrahedron* **1991**, *47*, 2649−2660.
(26) Kim, Y.; Kim, H. D.; Lee, Y. *J. Chem. Soc., Faraday Trans.* **1997**, *93*, 99−103.